

## APPENDIX

## Discussion of Eq. (5.3)

In the usual derivations, one obtains (5.2) having neglected terms in  $p^2$ . One then sets the denominator of (5.2) equal to a small quantity without investigating if the maximum permitted value for  $p$  is being exceeded. A more careful discussion can be based on the kinetic equation in the form

$$dp/dt = (T_2^* + T_4 p) [\gamma(N_A - N_D - p) - (N_D + p)] p, \quad (\text{A1})$$

where

$$\gamma \equiv (X_4 + X_2^*/p) / (T_2^* + T_4 p) \quad (\text{A2})$$

is usually taken to be independent of  $p$  near breakdown:

$$\gamma \approx X_4 / T_2^*.$$

In a steady state,

$$\frac{p}{N_A - N_D} = \frac{1}{1 + \gamma} \left[ \gamma - \frac{N_D}{N_A - N_D} \right]. \quad (\text{A3})$$

Approximate and simplified relations can be obtained in three steps:

(1) Breakdown usually occurs for  $p \ll N_A - N_D \sim 10^{15} \text{ cm}^{-3}$ . This is shown to be true by using Fig. 12 of Ref. 4 and the current density relation  $J = pe\mu F$  giving

$$10^9 \leq p \leq 10^{12} \text{ cm}^{-3}. \quad (\text{A4})$$

(2) From relation (4.2),  $T_2^* \sim 10^{-7} \text{ cm}^3/\text{sec}$ , while  $T_4 \leq 10^{-24} \text{ cm}^6/\text{sec}$  (Figs. 2 to 6 of Ref. 1) at low temperatures and if excited states can be neglected. Thus  $T_2^* \gg T_4 p$ ; hence (A3) simplifies to

$$[N_D / (N_A - N_D)] T_2^* \approx X_4 + X_2^*/p. \quad (\text{A5})$$

(3) From p. 1685 of Ref. 7,  $X_2^* \sim 10^{-2} \text{ sec}^{-1}$ , so that, using Fig. 5,  $X_2^*/p$  can be neglected in comparison with the other terms, thereby reducing (A5) to (5.3).

## Extrinsic Recombination Radiation from Natural Diamond: Exciton Luminescence Associated with the N9 Center

D. R. WIGHT AND P. J. DEAN\*

*Wheatstone Laboratory, King's College, Strand, London, England*

(Received 11 August 1966)

A luminescence system with no-phonon lines at 5.251 and 5.261 eV (at 100°K), observed in the edge luminescence spectra of natural diamonds containing relatively low concentrations of nitrogen in "platelet" form, has been identified with the so-called N9 center which is responsible for a well-known impurity-absorption feature. Evidence is presented supporting a recent identification of this absorption system with the creation of an indirect exciton bound to nearest-neighbor donor-acceptor pairs involving substitutional nitrogen donors and aluminium acceptors. The donor-acceptor pair behaves like a modified donor with reduced ionization energy, since the ratio of the ionization energies of the isolated donor and acceptor is approximately 10:1 and the donor binding energy is larger than the donor-acceptor interaction energy. The N9 absorption/luminescence system is only observed when the modified donor is neutral in the unexcited crystal. Comparison of the N9 absorption and luminescence spectra provides an unambiguous identification of the phonon replicas and of the principal no-phonon excited electronic states in the absorption spectrum. The one-phonon replicas have been studied in detail and are compared with those observed in a system involving excitons which are relatively weakly bound at neutral isolated aluminium acceptors in *p*-type semiconducting diamond. For both systems the exciton-phonon coupling is a maximum for the optical phonons of wave vector  $\mathbf{k}_c$  which conserve momentum in the intrinsic indirect transitions. The breadth and shape of the N9 optical-phonon replicas indicate, however, that coupling occurs for phonons with wave vectors distributed throughout at least the outer half of the reduced zone, whereas the replicas for the less tightly bound acceptor-exciton complex indicate that the coupling is negligible other than to phonons with wave vector relatively close to  $\mathbf{k}_c$ .

### I. INTRODUCTION

THE N9 system was first observed as an absorption center in natural diamonds some thirty years ago<sup>1</sup> and has since been investigated in absorption and luminescence excitation spectra by a number of workers.<sup>1-6</sup>

\* On leave of absence at Bell Telephone Laboratories, Murray Hill, New Jersey, U. S. A.

<sup>1</sup> R. Robertson, J. J. Fox, and A. E. Martin, *Phil. Trans. Roy. Soc. (London)* **A232**, 463 (1934).

This system has been shown to contain two strong sharp no-phonon lines at photon energies of 5.25 and 5.26 eV, a weaker line at 5.28 eV, and associated struc-

<sup>2</sup> F. A. Raal, *Proc. Phys. Soc. (London)* **24**, 649 (1959).

<sup>3</sup> K. S. Bai, *Proc. Ind. Acad. Sci.* **A19**, 253 (1944).

<sup>4</sup> K. G. Ramanathan, *Proc. Ind. Acad. Sci.* **A24**, 137 (1946).

<sup>5</sup> J. Nahum and A. Halperin, *J. Phys. Chem. Solids* **23**, 345 (1962).

<sup>6</sup> P. J. Dean and J. C. Male, *Proc. Roy. Soc. (London)* **A277**, 330 (1964).

ture at higher photon energies up to and beyond the indirect absorption edge of diamond at  $\sim 5.5$  eV. An interpretation of the  $N9$  absorption system in terms of the formation of an indirect exciton bound to a neutral nearest-neighbor donor-acceptor pair has recently been put forward<sup>7</sup> and the association of this center with another well-known absorption/luminescence feature ( $N3$ ) has been discussed.<sup>8</sup>

The present paper is concerned with luminescence from  $N9$  centers under electron-beam excitation. This luminescence has been observed previously,<sup>9</sup> but, owing to experimental inaccuracies, it was not realized that the structure observed was in fact luminescence from  $N9$  centers. A detailed comparison between the absorption and luminescence spectra associated with the  $N9$  center enables an unambiguous distinction to be made between the no-phonon and phonon-assisted spectral components. A recently studied near-band-edge extrinsic luminescence system in diamond involves indirect excitons bound to neutral aluminium acceptors.<sup>10</sup> Instructive differences and similarities between the latter spectrum and the  $N9$  luminescence spectrum are noted and discussed. Experimental evidence supporting the previously proposed interpretation of the  $N9$  luminescence<sup>7</sup> is also presented in this paper.

## II. EXPERIMENTAL

The luminescence was excited using an electron beam typically of 20  $\mu$ A and 60 keV. Electron-beam excitation is particularly suited to the study of near-band-gap-energy recombination radiation in diamond, since it is difficult to obtain a lamp and filter system which can produce a flux of  $\sim 6$  eV photons of sufficient intensity even for the detection of these emission bands at low resolution in photoluminescence.

The specimens were mounted on the copper nose of a stainless-steel Dewar which could be filled with a suitable refrigerant. Care was taken to ensure good and reproducible thermal contact between the specimens and the refrigerant bath. A small electric heater on the Dewar nose-piece facilitated measurements within about 100°K above the refrigerant temperature. A specimen temperature of about 50°K was obtained with the use of a Norelco helium circulating cryogenerator. The temperature in the immediate vicinity of the specimen was measured with a thermocouple. The temperature excess of the specimen over its immediate surroundings was estimated from the results of a previous experiment in which a thermocouple junction was placed in a small hole in a diamond which was then irradiated by the electron beam over a range of voltages and currents. The luminescence was analyzed using a Hilger E1 spec-

trometer modified for photoelectric detection with an E.M.I. type 6256 B photomultiplier.

## III. RESULTS AND DISCUSSION

### A. The Emission Spectrum

The luminescence at photon energies in the region of the absorption edge in diamond, obtained from a natural diamond (K.3) at 100°K, is shown in Fig. (1). The sharp lines  $X_0$  and  $X_0'$  have photon energies coinciding within experimental error with the pair of sharp lines near 5.26 eV which are characteristic of the absorption spectra of so-called intermediate type or type-I natural diamonds. Because of strong continuous absorption in the common type-I natural diamond due to the nitrogen platelets which are a characteristic property of these crystals<sup>11,12</sup> it is difficult to observe the  $N9$  system in absorption. However, this system may be conveniently studied in these crystals through its prominence in the edge excitation spectrum for visible luminescence.<sup>6</sup> Absorption measurements on thin plates ( $\lesssim 0.1$  mm thick) of type-I diamond which are difficult to prepare have confirmed the presence of strong  $N9$  system absorption in these crystals.<sup>13</sup> The  $X_0$  and  $X_0'$  luminescence lines have never been observed in an extensive survey of spectra from General Electric (U.S.A.) or De Beers (South Africa) synthetic diamonds, or from homogeneous natural semiconducting ( $p$ -type, so-called type-IIb) diamonds. Similarly the  $N9$  absorption system has not been observed in spectra from natural type-IIb diamonds or from any synthetic diamond.

It is therefore apparent that the spectrum shown in Fig. 1 is the luminescence version of the  $N9$  absorption system commonly found in natural diamond, and that lines  $X_0$  and  $X_0'$  represent no-phonon electronic transitions. The relatively broad bands  $Y_1$ ,  $X_1$ ,  $X_2$ , and  $X_3$  shown in Fig. 1 are discussed in Secs. III C and III D of this paper in terms of phonon replicas derived mainly from  $X_0$ .

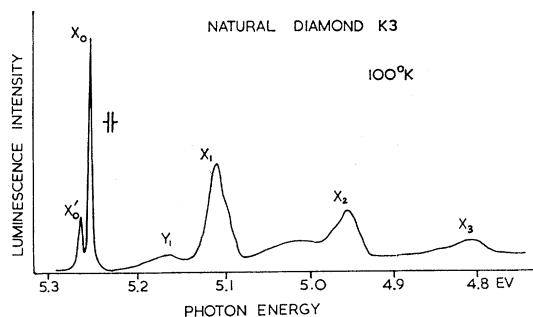


FIG. 1.  $N9$  luminescence from natural diamond K.3 (type I), resolution 0.003 eV.

<sup>7</sup> P. J. Dean, Phys. Rev. **139**, A588 (1965).

<sup>8</sup> P. A. Crowther and P. J. Dean (to be published).

<sup>9</sup> P. J. Dean and I. H. Jones, Phys. Rev. **133**, 1698 (1964).

<sup>10</sup> P. J. Dean, E. C. Lightowers, and D. R. Wight, Phys. Rev. **140**, A352 (1965).

<sup>11</sup> W. Kaiser and W. L. Bond, Phys. Rev. **115**, 857 (1959).

<sup>12</sup> T. Evans and C. Phaal, Proc. Roy. Soc. (London) **A270**, 538 (1962).

<sup>13</sup> F. A. Raal, Proc. Phys. Soc. (London) **74**, 647 (1959).

The luminescence system shown in Fig. 1 has only been observed from natural diamonds whose edge absorption and edge excitation spectra for visible luminescence indicated the presence of the  $N9$  centers without appreciable concentrations of nitrogen in platelet form. In fact no luminescence bands can be detected near the energy gap when the concentration of optically active nitrogen impurity is  $\gtrsim 10^{19}$  cm $^{-3}$  as commonly found both in natural diamond, where the nitrogen is mainly in platelets,<sup>12</sup> and in synthetic diamond, where the nitrogen is mainly in dispersed, paramagnetically active, sites.<sup>14,15</sup> As is to be expected from its electrical activity as a deep donor center, nitrogen in either form evidently provides an efficient competitive recombination process which does not involve either visible or ultraviolet luminescence.<sup>7</sup> These recombinations are therefore largely nonradiative. However, evidence will be presented in a later paper to show that electron-hole recombinations at associated (platelet) nitrogen as well as at dispersed nitrogen centers<sup>7</sup> give rise to efficient near infrared luminescence.

The  $N9$  transition is interpreted as the recombination of indirect excitons bound to neutral nearest neighbor donor-acceptor pairs, i.e., the radiative decay of  $\textcircled{5}DA_1$  centers using the notation of Ref. 7. The deep lying donor ( $E_D \sim 4$  eV) is thought to be substitutional nitrogen<sup>7</sup> and the acceptor ( $E_A \sim 0.37$  eV) has been identified with substitutional aluminium.<sup>10</sup> Impurity-activation analysis has shown that these impurities exist in significant amounts in all natural diamonds,<sup>16,17</sup> and are also thought to be the source, in associated form, of the blue "band A" luminescence of natural diamond and the green emission band of synthetic diamond.<sup>7</sup>

The identification of the  $N9$  system with transitions at a closely associated donor-acceptor center is consistent with the absence of these centers in synthetic diamonds, since the synthetic crystals do not contain the associated nitrogen complexes (platelets) which are common in natural diamonds. This difference in the degree of association of chemical impurities between natural and synthetic diamond is also supported by the spectral differences between the visible donor-acceptor pair luminescence.<sup>7</sup> Such a clear-cut and persistent difference presumably indicates that the growth conditions of natural and synthetic diamonds are very dissimilar. The absence of the  $N9$  system in natural semiconducting diamonds, which are  $p$ -type, supports the view that the center to which the exciton is bound has the character of a neutral donor, otherwise the visible luminescence spectra of these crystals would suggest that they generally contain a sufficient concentration of nearest-neighbor donor-acceptor pairs for the  $N9$  system to be detected.

<sup>14</sup> C. M. Huggins and P. Cannon, *Nature* **194**, 829 (1962).

<sup>15</sup> H. B. Dyer, F. A. Raal, L. du Preez, and J. H. N. Loubser, *Phil. Mag.* **11**, 763 (1965).

<sup>16</sup> E. C. Lightowers and P. J. Dean, (unpublished).

<sup>17</sup> E. C. Lightowers, *Anal. Chem.* **34**, 1348 (1962).

The  $\textcircled{5}DA_1$  complex involves an indirect exciton bound to a  $\textcircled{3}DA_1$  complex or neutral nearest-neighbor donor-acceptor pair, which can be treated as a "modified donor" center. The observed luminescence is thus extrinsic recombination radiation from excitons bound to neutral modified donor centers. It is instructive to compare it with the extrinsic near-band-gap recombination radiation observed from natural and synthetic semiconducting diamond. This luminescence is seen in Fig. 2 as observed from a natural specimen. The  $A$ ,  $B$ , and  $C$  features are intrinsic and are due to the recombination of free indirect excitons, whereas the  $D$  features are due to the decay of excitons bound to neutral aluminium acceptor centers ( $\textcircled{2}A$  centers).<sup>10</sup> The weak no-phonon  $D_0$  and  $D_0'$  emission consists of a sharp doublet whose splitting (12 meV) is slightly larger than that observed for the  $X_0$  and  $X_0'$  no-phonon lines (10 meV). In both systems this splitting is interpreted as the spin-orbit splitting of the exciton hole state which is perturbed from its value for the undisturbed lattice (7 meV), by the presence of the relevant impurity centers.<sup>18</sup> It is of interest that the luminescence spectra of nitrogen donors in silicon carbide exhibit the spin-orbit splitting of the hole state, which is of similar magnitude to the value for diamond, for exciton recombinations at *neutral* but not at *ionized* donor centers.

The one-phonon features  $D_1$ ,  $D_1'$ , and  $D_1''$  are much stronger and sharper relative to the no-phonon lines  $D_0$  and  $D_0'$  than in the  $X_1$  luminescence from  $N9$  centers, but the further phonon-assisted structure is successively broader and weaker in both luminescence systems. These points are discussed in Sec. III C. The binding energy of the exciton to the  $\textcircled{3}DA_1$  center is given by the energy difference between the position of the  $X_0$  and  $X_0'$  lines and the exciton energy gaps,<sup>10</sup> and is  $\sim 160$  meV.

### B. $N9$ No-Phonon Luminescence

In some fifteen diamonds where this luminescence has been observed it was evident that the relative intensities at a given temperature of the components  $X_0$  and  $X_0'$  varied only slightly from specimen to specimen, but the widths of these lines showed a marked variation. Usually the  $X_0'$  component was slightly broader than the  $X_0$  component. This line-width variation is accounted for by "frozen in" strains in the crystals. This has been confirmed by uniaxial stress experiments which show that  $X_0'$  is more sensitive to internal strain than  $X_0$ .<sup>19</sup> The no-phonon lines from a natural type-I crystal  $N1$  are shown at high resolution as a function of temperature in Fig. 3. This crystal showed the narrowest lines observed from the crystals studied.

The corrected half band width of  $X_0$  at 105°K is only  $\sim 0.8$  meV for crystal  $N1$ . This is of the same order

<sup>18</sup> D. R. Hamilton, W. J. Choyke, and L. Patrick, *Phys. Rev.* **131**, 127 (1963).

<sup>19</sup> P. A. Crowther (private communication).

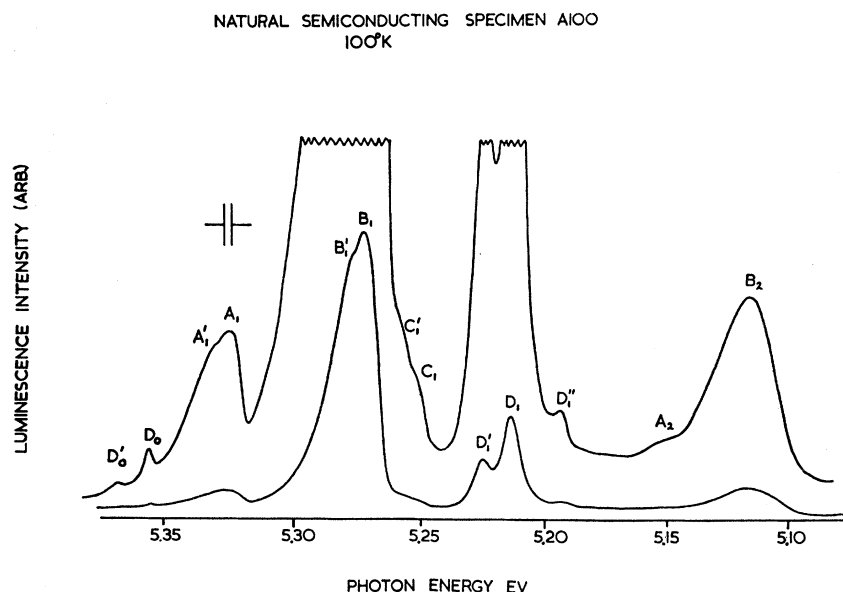


FIG. 2. Edge luminescence spectrum from natural *p*-type semiconducting diamond *A* 100. The upper trace was obtained at higher recording gain to show the weaker spectral features. Resolution 0.003 eV.

as the width of the sharpest lines in the photo-excitation spectrum of holes bound to the aluminum acceptor in the best available natural semiconducting diamonds. The minimum half bandwidths of the no-phonon lines in the many visible absorption/luminescence systems exhibited by natural diamonds are of the order of a few meV.<sup>8,20</sup>

Some of the residual broadening of the no-phonon lines is certainly due to interactions between the excited *N9* centers and other unexcited *N9* centers. Such broadening may be relatively important for weakly bound exciton states compared with the states associated with the deeper (visible) transitions, because of the relatively diffuse exciton wave functions of the shallow states. This interaction can lead to the hopping of the excitation energy between adjacent *N9* centers,

and thereby provides an efficient mechanism for the spatial transfer of the excitation to isolated centers with deep energy states.<sup>18,21</sup> This process can explain the quenching of the edge luminescence with increasing concentration of impurity centers which is apparent since the intermediate-type natural diamonds showing strong *N9* absorption generally do not show this system in luminescence. An extreme effect of this mechanism has been noted in the no-phonon lines of the *N9* system in luminescence excitation spectra of those natural diamonds which contain very high concentrations ( $\gtrsim 10^{20} \text{ cm}^{-3}$ ) of nitrogen and associated impurities. The no-phonon lines become so broadened for these crystals that the two components  $X_0$  and  $X_0'$  can no longer be mutually resolved. At the same time new and relatively sharp lines appear at lower energies, the most intense being at  $\sim 5.17 \text{ eV}$ .<sup>6</sup> Presumably these lower energy lines are due to the creation of excitons at more complex associated defects than the  $DA_1$  center. This broadening of the *N9* no-phonon lines is probably due to a reduction in the excited-state lifetime due to a very efficient transfer process to the deep centers.<sup>21</sup>

The limiting half-bandwidths observed for the lines  $D_0$  and  $D_0'$  attributed to the aluminium acceptor complex are also exceptionally small compared with those observed for the deeper transitions.

The detection of these narrow lines is favored in the luminescence of relatively weakly bound exciton states, since those inter-defect interactions which may lead to significant line broadening are also likely to reduce the luminescence efficiency below the level of detection. Such narrow luminescence lines are also more likely to be observed under electron-beam excitation of natural diamond crystals which often have strikingly inhomogeneous

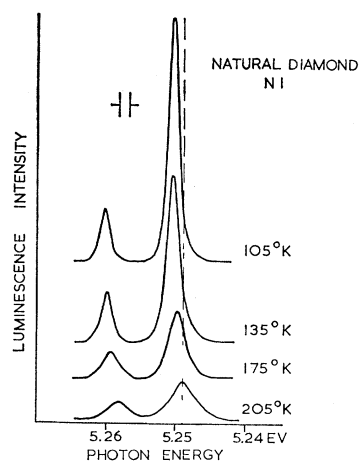


FIG. 3. *N9* no-phonon luminescence lines from natural diamond *N1* (type I). The traces are reproduced on the same intensity scale, for specimen temperatures between 105 and 205°K. Resolution 0.0014 eV.

<sup>20</sup> H. B. Dyer and I. G. Matthews, Proc. Roy. Soc. (London) A243, 320 (1957).

<sup>21</sup> D. G. Thomas and J. J. Hopfield, Phys. Rev. 150, 680 (1966).

geneous optical properties, since the excitation can be confined within a small volume  $\lesssim 10^{-6}$  cm<sup>3</sup>.

### 1. Relative Intensity Variation with Temperature

In common with the  $D_0$  components from semiconducting diamonds the ratio ( $\alpha$ ) of the intensity of the higher energy no-phonon luminescence line to that of the lower energy line decreases with decrease in specimen temperature. This is attributed in both cases to the thermalization of the hole populations in the split valence bands and follows the expression

$$\alpha = A \exp(E_s/kT), \quad (1)$$

where  $E_s$  is the relevant splitting,  $k$  is Boltzmann's constant,  $T$  is the temperature in °K, and  $A$  is the high-temperature limit of the ratio  $\alpha$ . The plot of  $\ln I_{x_0}'/I_{x_0}$  versus the reciprocal of the temperature is shown in Fig. 4. The slope is equivalent to a value of  $E_s = 10$  meV, which is the observed splitting of the doublet components. Points are included from two specimens measured, namely  $N1$  (linewidth  $\sim 0.8$  meV at 100°K) and  $K3$  (linewidth  $\sim 1.8$  meV at 100°K). From Fig. 4 the high-temperature limit of the ratio  $\alpha$  is  $0.85 \pm 0.05$ , compatible with the values obtained from luminescence excitation spectra, where thermalization does not occur, although this ratio is slightly specimen-dependent. The line at 5.28 eV seen in luminescence excitation is thought to be associated with the  $N9$  doublet. It has not been observed in the luminescence spectra, suggesting that it also derives from a splitting of the excited state of the transition, since such a weak line would not then be expected to appear in the low-temperature luminescence spectra because of thermalization of the excited-state populations.

### 2. Total Intensity Variation with Temperature

Careful measurements of the whole spectrum showed that the proportion of the total luminescence occurring in the no-phonon lines remained approximately constant between 50 and 250°K, so that the variation of the total luminescence intensity was measured from the integrated intensity of the no-phonon lines  $X_0$  and  $X_0'$

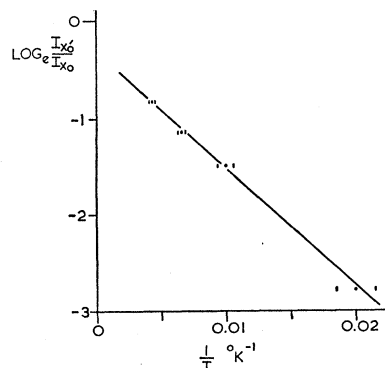
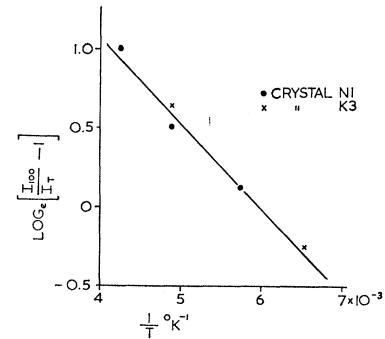


FIG. 4. Graph indicating the variation of the intensity ratio of the  $N9$  no-phonon lines with specimen temperature.

FIG. 5. Graph indicating the variation of the total intensity of the  $N9$  luminescence with specimen temperature. An activation energy for the observed variation is deduced from the slope of the graph (see text).



only. The results were fitted to the expression

$$\frac{I_T}{I_0} = \frac{1}{1 + C \exp(-E_I/kT)}, \quad (2)$$

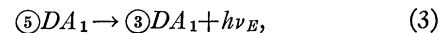
where  $I_T$  and  $I_0$  are the intensities at temperatures  $T$  and zero, respectively,  $C$  is a constant, and  $E_I$  the activation energy for the process investigated.

The graph shown in Fig. 5 is of  $\ln(I_{100}/I_T - 1)$  versus  $1/T$ , where  $I_{100}$  is the intensity at a temperature of 100°K. Since it was found that the intensity did not increase to any marked extent between 100 and 50°K, Eq. (2) can be approximated to

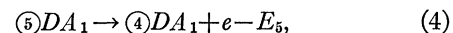
$$I_{100}/I_T - 1 = C \exp(-E_I/kT).$$

This approximation clearly becomes more accurate as  $I_{100}/I_T$  increases. From the slope of Fig. 5  $E_I$  was found to be  $36 \pm 7$  meV.

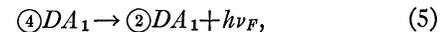
Since the transition is interpreted as:



where  $h\nu_E$  is the emitted photon energy, one might expect the value of  $E_I$  to coincide with the optically deduced exciton binding energy ( $\sim 160$  meV). However, an alternative decay process is apparent:



i.e., the  $\textcircled{5}DA_1$  complex can lose an electron, binding energy  $E_5$ , and become a nearest-neighbor donor-acceptor pair with an electron associated with the donor and a hole associated with the acceptor. This can then decay as



or the electron annihilates the hole on the acceptor with the emission of a photon (energy  $h\nu_F \sim 3$  eV<sup>8</sup>). The activation energy  $E_5$  has been calculated to be  $\sim 0.03$  eV from other sources<sup>8</sup> as compared to 0.16 eV for the thermal ionization of the exciton from the complex. The activation energy appropriate to the intensity dependence should be  $E_5$  as the observed value suggests, the concentration of  $\textcircled{5}DA_1$  complexes being governed by the decay process having the lowest activation energy.

### 3. Variation of Linewidth with Temperature

In Fig. 3 the widths of the components  $X_0$  and  $X_0'$  are seen to increase with temperature. Assuming the relationship

$$\Gamma_0^2 = \Gamma_s^2 + \Gamma^2, \quad (6)$$

where  $\Gamma_0$ ,  $\Gamma_s$ , and  $\Gamma$  are the widths at half-height of the observed line, mercury-discharge calibration line at the same resolution, and the true emission line, respectively; the true width of component  $X_0$  was calculated for a range of temperatures between 100 and 250°K. This relationship implies that the line measured was Gaussian in shape which was taken as a reasonable approximation. The linewidth  $\Gamma$  was found to vary as the square of the temperature in this range (Fig. 6).

Since the total heat energy in diamond varies as the fourth power of temperature in this region<sup>8</sup> the rms deviations of the lattice points would follow a square law with temperature, which thus may be reflected in the exciton-decay linewidth. Since the emission intensity falls rapidly with temperature it would be difficult to measure linewidths to higher temperatures to obtain more comprehensive data.

### 4. Variation of Line Position with Temperature

In Fig. 3 it is clear that the energies of the  $X_0$  and  $X_0'$  lines move to lower values as the temperature increases. The shifts observed follow those seen in luminescence excitation spectra accurately, and are of the same order as the shifts observed in the energy gap of diamond in this temperature range.<sup>22,23</sup> Clearly any variation in energy gap would be reflected in the photon energy of the exciton recombination for a relatively weakly bound exciton state, and thus these results are consistent with the interpretation envisaged.

### C. The One-Phonon Emission

Figure 7 shows the detailed shape of the one-phonon emission at 50°K. The peaks  $X_1'$  and  $X_1''$  are displaced from  $X_0$  by energies of  $141 \pm 1$  meV and  $163 \pm 2$  meV,

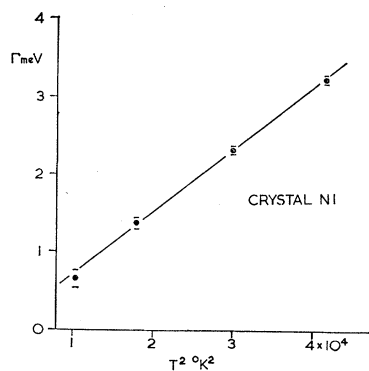


FIG. 6. Graph indicating variation of the half band width of the  $N_9$  no-phonon line  $X_0$ , with specimen temperature.

<sup>22</sup> J. C. Male, Ph.D. thesis, London University, London, 1962 (unpublished).

<sup>23</sup> C. D. Clark, P. J. Dean, and P. V. Harris, Proc. Roy. Soc. (London) **A277**, 312 (1964).

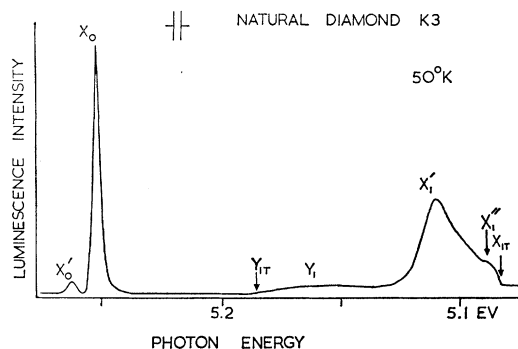


FIG. 7. No-phonon and one-phonon-assisted regions of the  $N_9$  luminescence spectrum at 50°K. Resolution 0.003 eV.

respectively. These energies represent the favored phonons for one-phonon-assisted transitions and are in excellent agreement with those associated with the extrinsic components  $D_0$ ,  $D_1'$ , and  $D_1''$  from semiconducting diamond (Fig. 2). These phonons conserve crystal momentum for indirect interband transitions and are selected from the transverse optical (141-meV) and longitudinal optical (163-meV) branches.<sup>10</sup> Since  $X_0'$  is very weak compared with  $X_0$  at 50°K, the one-phonon-assisted luminescence corresponding to  $X_0'$  is not apparent.

The intensity of the one-phonon luminescence relative to the no-phonon luminescence is very much larger for the  $D$  features than for the  $X$  features, and the widths of the one-phonon peaks from the  $(5)DA_1$  centers are appreciably larger than those from  $(4)A$  centers. Thomas *et al.*<sup>24</sup> suggested that the free exciton-phonon selection rules should be obeyed for sufficiently weakly bound indirect excitons, i.e., the crystal momentum-conserving phonons for indirect transitions across the energy gap should be selected for the one-phonon emission. Further it is suggested that as the binding becomes stronger, the no-phonon transition, initially forbidden, should become more prominent, the one-phonon transitions should become weaker, and the phonon selection rules should become relaxed. Phonons will then be selected on density-of-lattice states or local-mode criteria.

These effects are clearly present on comparing the  $D$  luminescence from  $(4)A$  centers (weakly bound exciton  $\sim 50$ -meV binding energy) and the  $X$  luminescence from  $(5)DA_1$  centers (exciton binding energy  $\sim 160$  meV). Similar contrasts have been observed in the comparison of the  $(4)D$  and  $(3)D$  luminescence spectra of nitrogen donors in silicon carbide,<sup>18</sup> where neither system can be observed in absorption. Failure to observe components analogous to  $D_0$  and  $D_0'$  in the absorption spectra of semiconducting diamond, although  $X_0$  and  $X_0'$  can readily be seen in absorption spectra of intermediate-type natural diamond, is due to the following factors. (a) The oscillator strength of the no-phonon line for the more diffuse, lower binding energy, indirect exciton state is less because the spreading of the exciton wave

<sup>24</sup> D. G. Thomas, M. Gershenzon, and J. J. Hopfield, Phys. Rev. **131**, 2397 (1963).

function in momentum space is less, giving a smaller admixture of the direct band-gap wave function which makes the transition allowed. (b) Natural semiconducting diamonds may be  $\gtrsim 5$  mm thick but contain typically  $\gtrsim 5 \times 10^{16} \text{ cm}^{-3}$   $\textcircled{2}A$  centers<sup>10</sup> whereas the concentration of  $N9$  centers is probably much higher in many crystals. The concentration of  $\textcircled{2}A$  centers may be  $\sim 100\times$  greater in doped synthetic diamonds,<sup>10</sup> but the useable thickness of these crystals is generally  $< 0.5$  mm.

The spectral position of the weakly bound exciton system is such that the relatively strong phonon-assisted components occur appreciably above the threshold for continuous absorption due to intrinsic transitions. Absorption bands due to  $\textcircled{4}D$  or  $\textcircled{4}A$  exciton complexes have not been observed in silicon or germanium, although the luminescence of these centers is well known.<sup>25,26</sup>

A significant difference between the nature of the phonon cooperation in the aluminum  $\textcircled{4}A$  system and the  $N9$  system may be anticipated since the localization energy of the exciton in the  $\textcircled{4}A$  system ( $\sim 50$  meV) is considerably less than the internal binding energy  $E_x$  of the free exciton, whereas the reverse is true for the  $N9$  system. Similar considerations apply to the  $\textcircled{4}D$  and  $\textcircled{3}D$  nitrogen complexes in silicon carbide.<sup>18</sup>

There is no simple quantitative theory for the change in phonon cooperation occasioned by a given change in the total binding energy of the electron and hole of the exciton. Some qualitative comments may be made, however, in the light of a comparison between the experimental spectrum shown in Fig. 7, and the lattice dispersion curves for diamond.<sup>27</sup> It is notable that the high-energy threshold of component  $X_1'$  in Fig. 7 corresponds to a phonon energy of  $\sim 130$  meV, close to the low-energy cutoff for the transverse optical branch at the  $\langle 100 \rangle$ -type reduced zone boundaries.<sup>27</sup> The well-defined low-energy cutoff shown as  $X_{1T}$  in Fig. 7 gives a phonon energy of  $167 \pm 1$  meV in reasonable agreement with the high-energy cutoff for the optical branches at the zone center (Raman energy). Component  $Y_1$  of Fig. 7 has a high-energy threshold corresponding to a phonon energy of  $\sim 65$  meV, close to the energy of the maximum density of states for the  $\langle 111 \rangle$ -type transverse acoustical phonon branches. There is a decrease in coupling to the acoustical phonons for energies  $\gtrsim 100$  meV, which is the energy of the density-of-states maximum for  $\langle 100 \rangle$ -type transverse acoustical phonons.<sup>27</sup> The ratio of the total coupling to acoustical and optical phonons for the  $N9$  center is  $\sim 0.15$  and is much larger than the limiting value of  $< 0.005$  found for the  $\textcircled{4}A$  center where acoustical phonon replicas have not been observed.

<sup>25</sup> J. R. Haynes, Phys. Rev. Letters 4, 361 (1960).

<sup>26</sup> C. Benoit a la Guillaume and O. Parodi, in *Proceedings of the International Conference on Semiconductor Physics, 1960* (Czechoslovakian Academy of Sciences, Prague, 1961), p. 426.

<sup>27</sup> J. L. Warren, R. G. Wenzel, and J. L. Yarnell, International Symposium on the Inelastic Scattering of Neutrons, Bombay, 1964 (unpublished); see also Ref. (10).

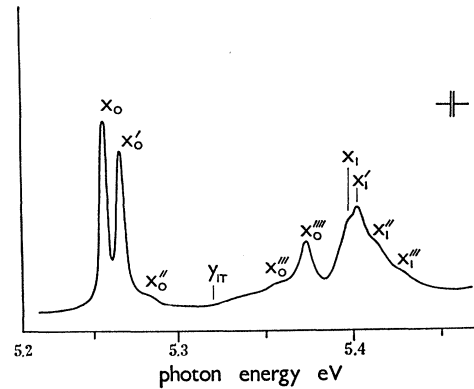


Fig. 8. Edge excitation spectra for visible luminescence, from specimen P13 (intermediate type). Specimen temperature  $80^\circ\text{K}$ , resolution  $0.002$  eV. Comparison of the phonon-assisted region with that seen in luminescence emission enables the participating phonons to be identified. (See text.)

We can therefore conclude that the increased localization of the exciton at the  $N9$  center compared with the  $\textcircled{2}A$  center leads to enhanced interaction with acoustical phonons, probably because of the significant reduction of the magnitude of the exciton diameter compared with the wavelengths of the acoustical modes at the density-of-states maxima of the phonon distribution. The optical replicas suggest that the exciton-phonon interaction is significant for a range of wave vectors extending at least over the outer half of the reduced zone.

Confirmation that the bands labeled  $Y_1$ ,  $X_1'$  and  $X_1''$  in Fig. 7 are phonon replicas of  $X_0$  is obtained from a comparison with Fig. 8 which shows the details of the  $N9$  absorption spectrum. Additional fine structure is observed in the optical-phonon replica because of the presence of no-phonon lines  $X_0$  and  $X_0'$  with comparable intensities in absorption. Figures 7 and 8, and the energies listed in Table I show that the optical replicas in the absorption and luminescence spectra exhibit mirror symmetry about the no-phonon lines. The symmetrical broadened absorption line at  $\sim 5.37$  eV does not have a counterpart in the luminescence spec-

TABLE I. Comparative analysis of  $N9$  absorption and luminescence spectra.

Band	Absorption ( $80^\circ\text{K}$ )		Luminescence ( $100^\circ\text{K}$ )	
	Energy (eV) <sup>a</sup>	Identification <sup>b</sup>	Energy (eV) <sup>a</sup>	Identification <sup>b</sup>
$X_0$	$5.254 \pm 0.002 (P)$	No-phonon	$5.251 \pm 0.001 (P)$	No-phonon
$X_0'$	$5.263 \pm 0.002 (P)$	No-phonon	$5.261 \pm 0.001 (P)$	No-phonon
$X_0''$	$5.280 \pm 0.002 (P)$	No-phonon	...	...
$Y_{1T}$	$5.319 \pm 0.002 (T)$	$X_0 + \hbar\omega_{TA}$	$5.185 \pm 0.002 (T)$	$X_0 - \hbar\omega_{TA}$
$X_0'''$	$5.355 \pm 0.002 (P)$	No-phonon	...	...
$X_0''''$	$5.372 \pm 0.002 (P)$	No-phonon	...	...
$X_1$	$5.395 \pm 0.002 (S)$	$X_0 + \hbar\omega_{TO}$	$5.110 \pm 0.001 (P)$	$X_0 - \hbar\omega_{TO}$
$X_1'$	$5.402 \pm 0.002 (P)$	$X_0' + \hbar\omega_{TO}$	...	...
$X_1''$	$5.413 \pm 0.003 (S)$	$X_0 + \hbar\omega_{LO}$	$5.088 \pm 0.002 (S)$	$X_0 - \hbar\omega_{LO}$
$X_1'''$	$5.247 \pm 0.003 (S)$	$X_0' + \hbar\omega_{LO}$	...	...
$X_{1T}$	...	...	$5.084 \pm 0.001 (T)$	$X_0 - \hbar\omega_R$
$X_{2T}$	...	...	$4.923 \pm 0.003 (T)$	$X_0 - 2\hbar\omega_R$
$X_{3T}$	...	...	$4.764 \pm 0.005 (T)$	$X_0 - 3\hbar\omega_R$

<sup>a</sup> Mean values:  $\hbar\omega_{TA} = 65$  meV;  $\hbar\omega_{TO} = 141$  meV;  $\hbar\omega_{LO} = 163$  meV;  $\hbar\omega_R = 166$  meV. (P) denotes peak, (T) threshold, (S) shoulder.

<sup>b</sup> TA=transverse acoustical. TO=transverse optical. LO=longitudinal optical.

trum, however, and apparently represents a no-phonon excited electronic state of the bound exciton. It is notable that this line broadens more rapidly than  $X_0$  and  $X_0'$  as the temperature is increased from 100 to 400°K, presumably due to a decrease in the excited-state lifetime arising from enhanced dissociation by phonon interactions. There is a low-energy threshold near 5.35 eV for the acoustical phonon optical absorption replicas, again corresponding to a phonon energy of 65 meV. The well-defined threshold near 5.35 eV in Fig. 8 does not have a counterpart in the emission spectrum of Fig. 7 and is therefore attributed to a no-phonon absorption line in Table I. The high-energy cutoff at the Raman energy above  $X_0$  and  $X_0'$  is not as well defined in absorption as it is in luminescence probably because it is obscured by transverse optical replicas of the no-phonon line at  $\sim 5.28$  eV.

#### D. Multiple Phonon Bands

These bands  $X_2$  and  $X_3$  in Fig. 1 show no fine structure, and since there are no longer any selection rules relevant to the emission of a second or third phonon this is to be expected. However, the low-energy thresholds indicate that successive Raman phonons are selected in the limiting case (Table I). The multiple phonon optical absorption replicas of the  $N9$  system are distorted by overlap with the intrinsic interband absorption processes.<sup>3</sup>

#### E. Other Luminescence Features

The broad band near 5.02 eV in Fig. 1 may be due to a residual amount of damage in the crystal since a

sharp line and band system ( $1D$ ) which contributes luminescence in this region is often seen in specimens showing  $N9$  luminescence and was observed extremely strongly in an artificially damaged specimen.

The connection between the  $1D$  system and lattice damage will be the subject of further experiment.

#### IV. CONCLUSIONS

The recently proposed interpretation for the  $N9$  system has been seen to be consistent with the transitions observed in luminescence. The luminescence has been attributed to the recombination of excitons bound to nitrogen-aluminium nearest-neighbor pairs. Phonon replicas have been identified by a comparison of the  $N9$  absorption and emission spectra. Some of the phonon energies thereby deduced are consistent with those known to be selected in indirect interband transitions. The effects of the relatively large exciton binding energy in the  $N9$  center compared with an exciton complex involving aluminium acceptor centers are shown to be qualitatively similar to those observed in other Group IV crystals.

#### ACKNOWLEDGMENTS

We would like to thank W. F. Cotty (Industrial Distributors, London) and Dr. F. A. Raal (Diamond Research Laboratory, Johannesburg) for providing many of the specimens used in this work. We are also grateful to Dr. J. C. Male for permitting the publication of Fig. 8. One of us (D.R.W.) is indebted to the Science Research Council for the provision of a maintenance grant.

### Electroreflectance at a Semiconductor-Electrolyte Interface\*

MANUEL CARDONA, KERRY L. SHAKLEE, AND FRED H. POLLAK

*Physics Department, Brown University, Providence, Rhode Island*

(Received 28 July 1966)

The electroreflectance spectra of Si, Ge,  $\alpha$ -Sn, AlSb, GaP, GaAs, GaSb, InP, InAs, InSb, ZnO, ZnTe, CdS, CdSe, and CdTe are reported. The measurements were performed by the electrolyte technique in the 1- to 6-eV photon energy range. The data were processed by the Kramers-Kronig technique and the variation in  $\epsilon_1$  and  $\epsilon_2$  induced by the applied electric field obtained. Several sharp peaks were observed in all these spectra and interpreted in terms of critical points in the joint density of states for optical transitions. As a result, a large number of direct interband energy gaps and spin-orbit splittings is obtained. These spin-orbit splittings are interpreted and correlated by using the  $\mathbf{k} \cdot \mathbf{p}$  method: Enough experimental information is available to determine the effects of spin-orbit interaction on the valence bands of most of these materials at any point in  $\mathbf{k}$  space.

#### I. INTRODUCTION

**M**ODULATION techniques have been employed recently in optical reflection and absorption measurements of solids to achieve greater sensitivity

and resolution. All these techniques have, as a common feature, the application of a small perturbation such as a change in lattice constant or an external field which destroys some invariant property of the crystal structure. The perturbation is made sinusoidally dependent on time, and thus a sinusoidal modulation of the response of the sample material to optical excitation is

\* Supported by the National Science Foundation and the U. S. Army Research Office, Durham.